08

1D Chains of composite nanoparticles graphene : h-BN and fluorinated graphene : V_2O_5 on a nanostructured polimer surface

© I.V. Antonova[1,2], V.A. Seleznev[1], N.A. Nebogatikova[1], A.I. Ivanov[1], V.S. Tumashev[1]

[1] Rzhanov Institute of Semiconductor Physics, Siberian Branch, Russian Academy of Sciences, Novosibirsk, Russia
[2] Novosibirsk State Technical University, Novosibirsk, Russia

E-mail: antonova@isp.nsc.ru

Received December 7, 2023
Revised January 15, 2024
Accepted January 28, 2024

The structures formed by applying suspensions of composite nanoparticles onto grating of an array of extended grooves formed using imprint nanolithography on the polymer surface were studied. Fluorinated graphene (FG)-coated V_2O_5 nanoparticles or graphene (G) : h-BN composite nanoparticles were deposited on the polymer using 2D printing. It has been shown that treatment of polymer grating with oxygen plasma, or additional sputtering and removal of a gold layer modify the surface properties and make it possible to organize various options for the assembly of nanoparticles on a structured polymer surface. Without treatment, the surface of the grating is hydrophobic and nanoparticles practically do not interact with it. Treatment with oxygen plasma led to the formation of a layer of nanoparticles over the entire surface of the grating, primarily filling the nanogrooves. Long-term activation was achieved by sputtering gold followed by mechanical removal using an adhesive transfer method. In the case of long-term surface activation, nanoparticles are located exclusively on the upper part of the polymer strips, practically without reducing the depth of the grating relief. FG : V_2O_5 particles are located in the middle of the polymer strips (nanocrests), while G : h-BN formed two 1D chains of nanoparticles along the edges of the ridge.

Keywords: imprint lithography, polymer grating, long-term activation, nanoparticles, 1D chains, electrical properties.

DOI: 10.61011/PSS.2024.03.57941.270

1. Introduction

Flexible (stretchable, wearable) electronics includes a whole class of electronic devices of various types that have the capacity to withstand a certain level of mechanical impact (bending, rolling, stretching) and retain their functional properties. It is expected that flexible electronics will be used in the near future in all kinds of gadgets, touch screens, sensors, a wide range of medical devices, and communication and Internet devices [1–5]. The progress in flexible electronics is associated with rapid advances in straintronics, which is a relatively novel line of research in condensed matter physics that focuses on the use of strain engineering methods and strain-induced physical effects in solids in the design of advanced information, sensor, and energy-saving equipment [5,6].

Nanostructured substrates offer a unique opportunity to design structures based on nanoparticles with controlled properties and distribution. Choosing specific substrate/nanoparticle combinations and techniques for structure fabrication and processing, one may set the range of possible applications of structures in nanoelectronics (metamaterials, plasmonic materials), biosensorics, or medicine [7–9]. It should be noted that the process of nanostructuring of substrates allows one to produce (specifically, by introducing local strain) regions that differ in their chemical activity. In addition, strain often contributes to an enhancement of the adsorption capacity of local regions by lowering energy barriers [10]. Specifically, the authors of [11] have discussed the technique of selective deposition of a thin transition metal layer that induces strain and stimulates the growth of islands on plasmonic metal nanoparticles. This is a novel strategy for engineering of unique morphologies that are hard to implement via traditional processes. A similar simple and economically viable method for selective nanoparticle deposition was used to fabricate sensors based on carbon nanofiber [12].

In the present study, the conditions of formation and the properties of one-dimensional chains of functional nanoparticles on a grating made from a polycarbonate-based material were determined: V_2O_5 particles decorated with fluorinated graphene (FG) for memristors and composite graphene (G)–hexagonal boron nitride (h-BN) particles formed chains on grating nanoridges with V_2O_5/FG positioned in the middle of a ridge (at its crest) and G : h-BN arranged along its edges.

2. Methods of fabrication and examination of structures

Sets of gratings with a width of 80 nm, a depth of 150 nm, and a period of 180 nm were fabricated by nanoimprint

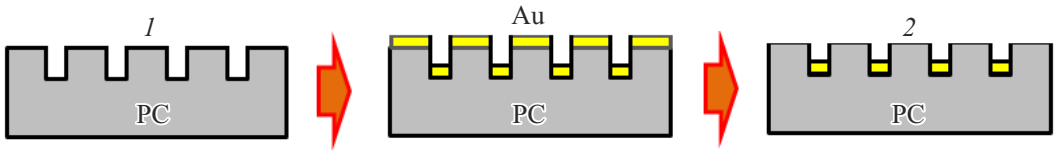

Figure 1. Schematic diagrams: *1* — grating fabricated by imprint lithography on a substrate made of a polycarbonate-based material and *2* — grating with its surface activated by sputtering and mechanical removal of a gold layer.

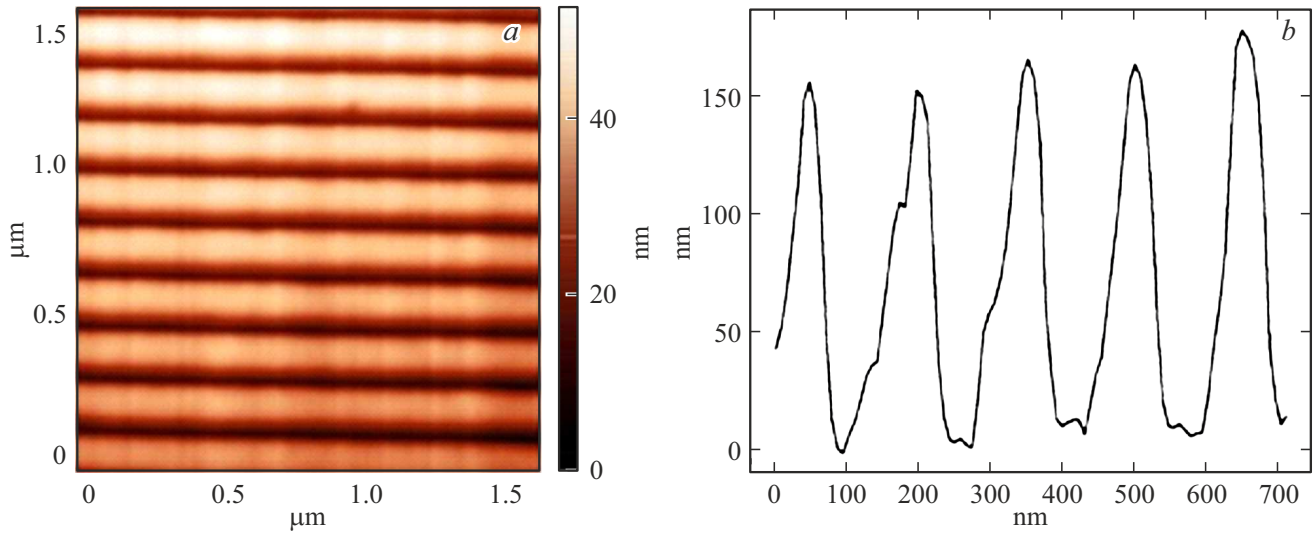

Figure 2. *a* — AFM image of the polymer grating surface after sputtering of a 30-nm-thick Au layer and its removal from the top (ridges) of the grating (the groove depth is 150 nm, and the period is 180 nm); *b* — surface relief across grating grooves, which verifies the formation of a surface pattern with expected parameters.

lithography on the surface of a polymer substrate (IPS polycarbonate-based material, Obducat, Sweden). The fabrication procedure was discussed in more detail in [13].

Two methods of surface activation for adjusting the adhesion between polymer grating and nanoparticles were used. In the first case, processing in oxygen plasma with a power of 100 W and a duration of 12 and 30 s was performed.

In the second case, a gold layer ~ 30 nm in thickness was sputtered onto the grating, and gold was then removed from the top (i. e., nanoridges) of the grating by adhesive transfer [13] (see Figure 1). It was found by examining the conductivity of the obtained grating that its top part is non-conducting, while gold nanostrips at the bottom of grooves have a resistance of 150–300 Ohm/□ measured along the strip. Thus, as far as electric conductivity is concerned, gold is removed completely from the top of the grating. In what follows, these substrates are called activated ones. An atomic force microscopy (AFM) image of such a grating is presented in Figure 2. It was found that, in terms of surface activation, the properties of these substrates remain unchanged for several months, making them suitable for nanoparticle deposition.

Two types of nanoparticles were used in this study. (1) V_2O_5 nanoparticles ~ 5 nm in size were prepared by sol-gel synthesis [14]. Fluorinated graphene was obtained by fluorinating graphene particles (100–300 nm in size with a thickness up to 5 nm) produced via exfoliation of natural purified graphite particles in an aqueous solution of hydrofluoric acid [15]. Additional exfoliation and particle size reduction occur in the process of fluorination; the resulting FG size was 30–50 nm at a thickness up to 2 nm [16]. Suspensions of V_2O_5 and FG in a solution of ethanol in water (70 : 30%) with a particle content of 1 mg/ml were then prepared. Composite nanoparticles were produced by mixing FG and V_2O_5 particle suspensions at the ratio of 1 : 1 and subjecting them to ultrasonic treatment. Owing to fine adhesion, fluorinated graphene decorated V_2O_5 particles, forming FG : V_2O_5 composite nanoparticles with a hydrophilic surface. It has been demonstrated earlier that such nanoparticles are capable of resistive switching, which makes them promising candidates for memristor fabrication [17].

Composite nanopartcles of the second type were produced from graphene particles (100–150 nm in size with a thickness up to 2 nm) and hexagonal boron nitride particles (20–50 nm in size with a thickness up to 2 nm) synthesized in plasma. The ratio of components in the composite suspension was 1 : 1, and the mass fraction of particles in the initial suspensions was 1 mg/ml. The properties

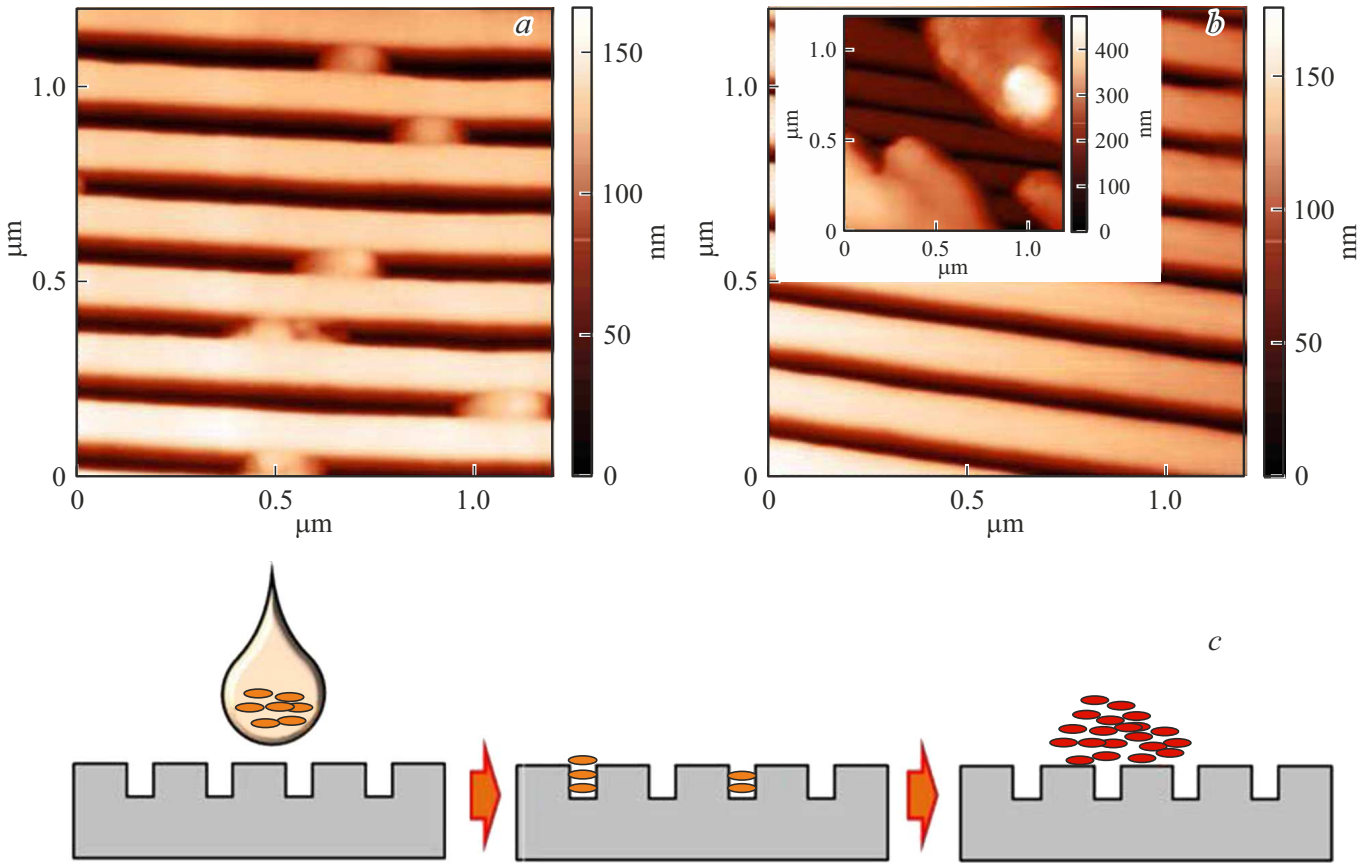

Figure 3. AFM images: *a* — FG:V_2O_5 particles in grooves of a non-activated grating and *b* — G:h-BN particles on this initial grating. The AFM image with a different scale and large particle clusters is shown in the inset. *c* — Schematic view of a non-activated grating with particles deposited onto it.

of these particles were discussed in more detail in [18]. Polar hexagonal boron nitride particles play a significant part in G:h-BN. They are responsible for rapid cluster formation and, most likely, govern the interaction with the substrate. The lateral size of composite particles is 80–90 nm, and their thickness is 10–15 nm.

Composite G:h-BN or FG:V_2O_5 particles were deposited onto the initial and activated nanostructured surfaces of polymer substrates by 2D printing. The printing technique provided an opportunity to form a thin even nanoparticle layer. The number of printed layers varied from 1 to 3. A Dimatix FUJIFILM DMP-2831 inkjet printer was used. The diameter of a printing droplet was $\sim 50\,\mu$m, and the printed area was several square millimeters in size.

A Solver PRO NT-MDT atomic force microscope was used to image the surface of studied films and study the surface relief. Measurements were performed in contact and semi-contact modes. The electric characteristics of prepared films were studied using JANDEL four-point probe equipment and an HM21 test unit at room temperature (Jandel Engineering Limited, United Kingdom). Current–voltage curves were also measured with a Keithley 6485 picoammeter for samples fitted with two silver contacts.

3. Experimental results

If one takes an initial structured (non-activated) substrate and performs particle deposition, it becomes evident that particles do not interact with the grating: either suspension drips down into grooves (FG:V_2O_5) or form relatively large particles (clusters), which „ignore“ structuring, simply form on the grating surface. The AFM data are shown in Figure 3.

The key feature of deposition of FG:V_2O_5 nanoparticles onto a surface activated by oxygen plasma is the interaction of particles with the grating and filling of grating grooves. Specifically, the profile corresponding to line *1* in Figure 4, *a*, which is drawn across the grating nanogrooves, indicates a depth of 40–50 nm instead of the initial depth of 150 nm (Figure 4, *b*). The profiles corresponding to lines *2* and *3* in Figure 4, *a*, which are drawn along the bottom of a nanogroove and along the crest of a nanoridge, have a relief of 15–20 nm and 6–8 nm, respectively. The observed relief is likely shaped by nanoparticles that fill the entire surface (most particularly, grooves). The examination of electric properties of the deposited film revealed zero conductivity. A similar result was obtained when the second (less intense) regime of plasma processing at 100 W for 12 s was used.

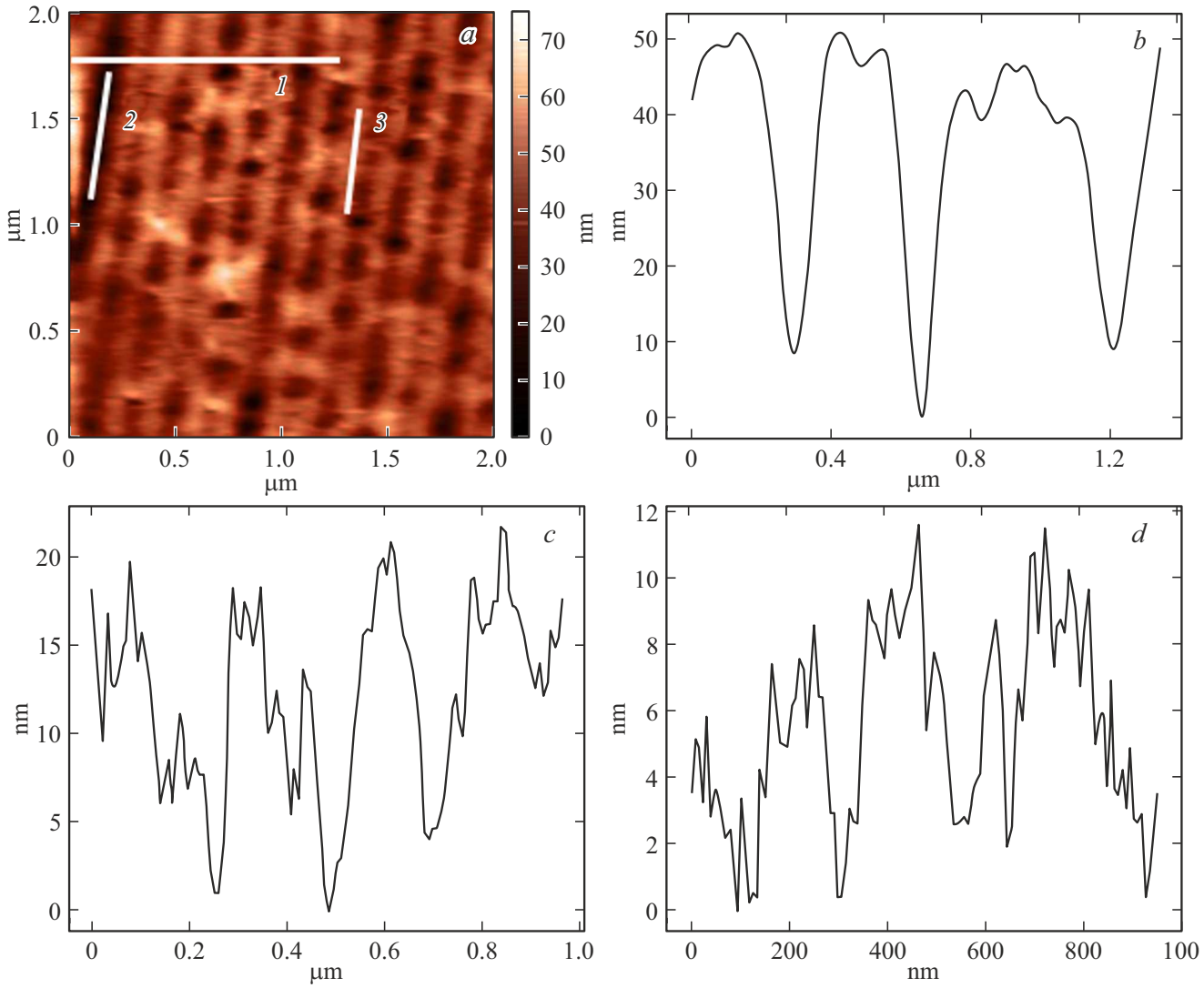

Figure 4. *a* — AFM image and *b, c, d* — surface relief of a grating after activation in plasma (100 W, 30 s) and FG : V_2O_5 particle deposition. Surface relief: *b* — along line *1*, *c* — along line *2*, and *d* — along line *3*.

The interaction character changed after activation of the polymer grating by sputtering and removal of a gold layer. According to the AFM data, 2D-printed nanoparticles are positioned exclusively at the crests of nanoridges and do not reduce the depth of grating nanogrooves.

Let us examine the results of deposition of composite FG : V_2O_5 particles onto a nanostructured surface in more detail. When a single suspension layer was printed, the AFM image (Figure 5) reveals individual nanoparticles or their clusters 10 nm in height positioned at the nanocrests. When three particle layers were printed, a denser layer covering the grating nanoridges was formed (see Figure 6). The transverse profile (Figure 6, *b*) demonstrates that the height of nanoridges (or the depth of nanogrooves) increased by approximately 10 nm. In view of this, the AFM probe provides worse resolution at the bottom of nanogrooves. The surface profile along the crest of a grating nanoridge (Figure 6, *d*) suggests that nanoparticles and their clusters have a lateral size of 80–90 nm and a thickness of 8–12 nm and form one-dimensional chains at the crests of ridges.

FG : V_2O_5 layers demonstrate two-level resistive switching with low voltages of 0.005–0.04 V (see Figure 7). Similar effects (switching voltage reduction to 0.1–0.5 V and the emergence of 2–3-level switching) were observed for crossbar structures with thin (1–2 particle monolayers) active FG : V_2O_5 layers on unstructured substrates. The structuring of substrates resulted in a further switching voltage reduction, which is likely attributable to the formation of 1D chains of FG : V_2O_5 particles.

Next, we examine the deposition of composite G : h-BN particles by printing onto an activated grating surface. Figure 8 presents images of the surface of nanostructured substrates with G : h-BN nanoparticle layers deposited by 2D inkjet printing. The profile of a transverse section of a nanostructured substrate with a G : h-BN nanoparticle layer formed by triple-pass printing is shown in Figure 9.

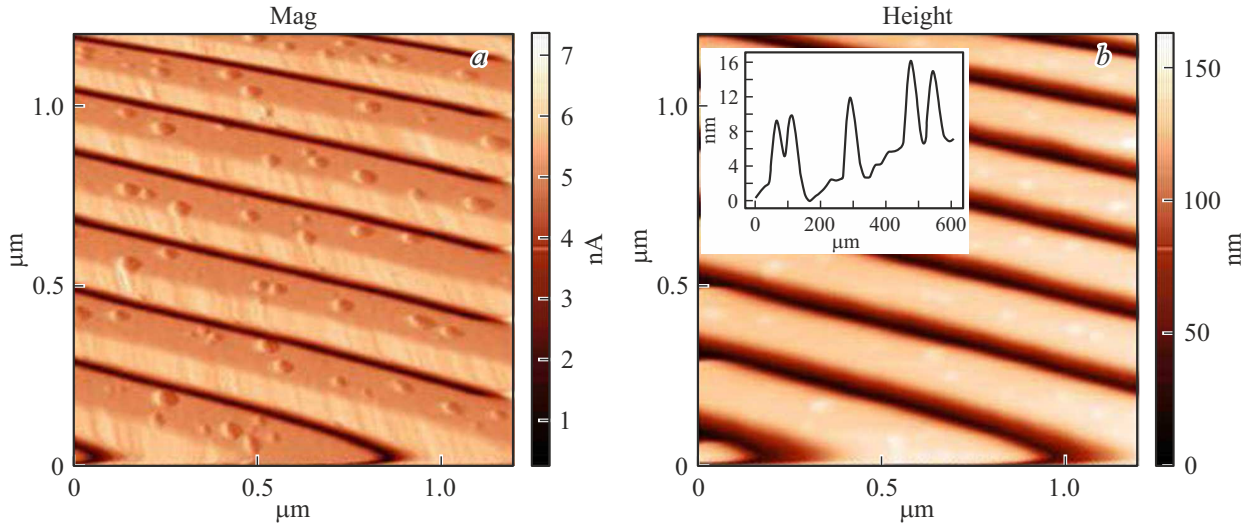

Figure 5. AFM images of the surface of an activated grating after deposition of a single layer of FG:V_2O_5 nanoparticles in *a* — Mag and *b* — surface relief modes. A typical profile along the crest of a ridge is shown in the inset. Individual nanoparticles with a height of 10 nm are discernible.

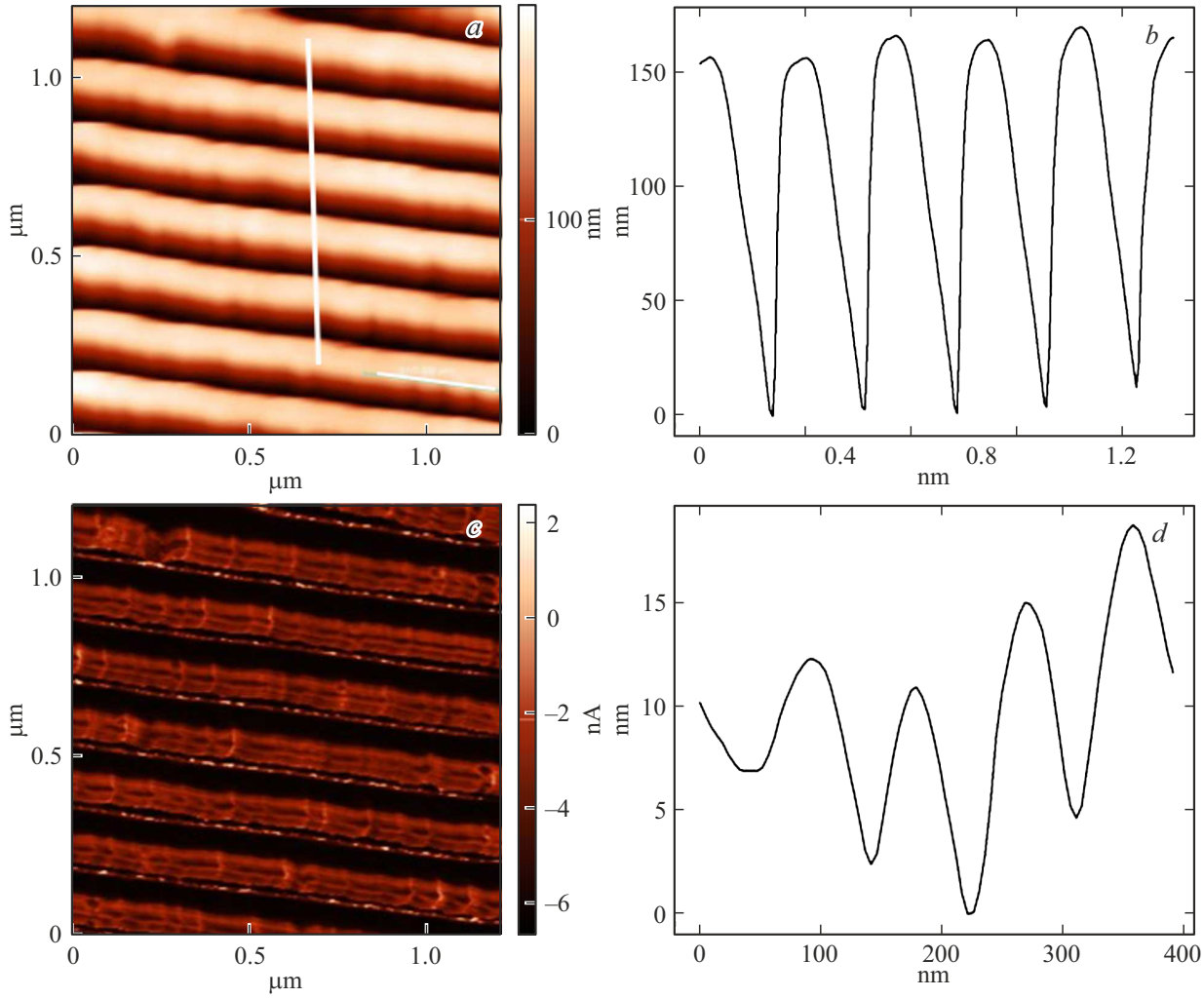

Figure 6. *a* — AFM image and *c* — Mag*Sin image of the surface of a nanostructured substrate with deposited FG:V_2O_5 particles; (*b*, *d*) — surface profiles across nanogrooves (*b*) and along the crest of a nanoridge (*d*) that correspond to white lines in the upper left panel.

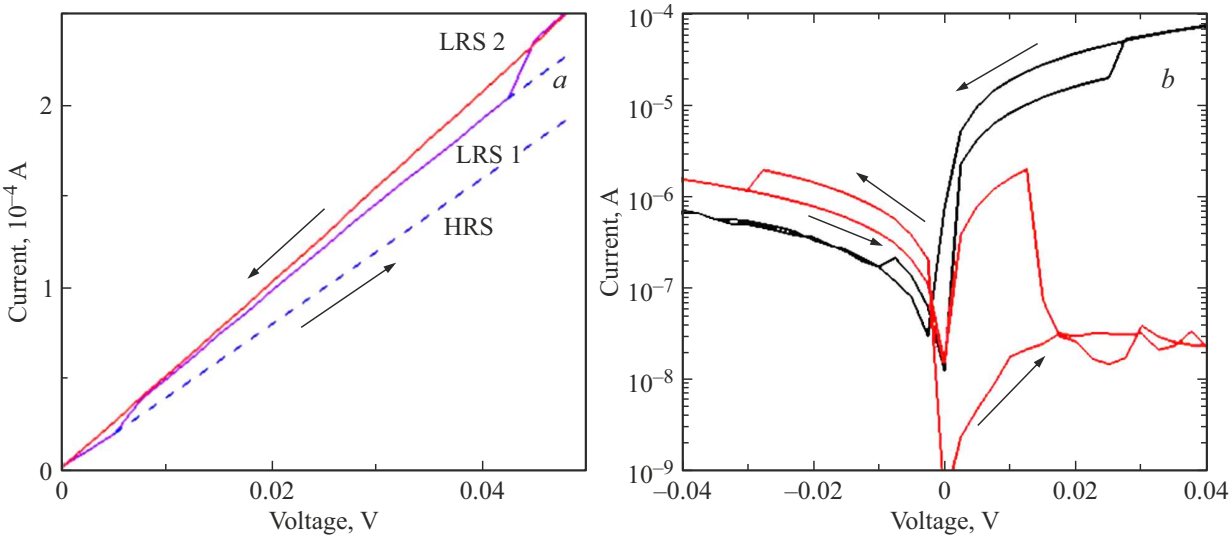

Figure 7. Switching observed along FG : V_2O_5 nanoparticle chains formed on the grating by 2D printing: *a* — single-pass FG : V_2O_5 nanoparticle printing, *b* — triple-pass FG : V_2O_5 nanoparticle printing. Voltage was applied between Ag contacts on the grating surface; different curves in the right panel correspond to different contact pairs on the surface.

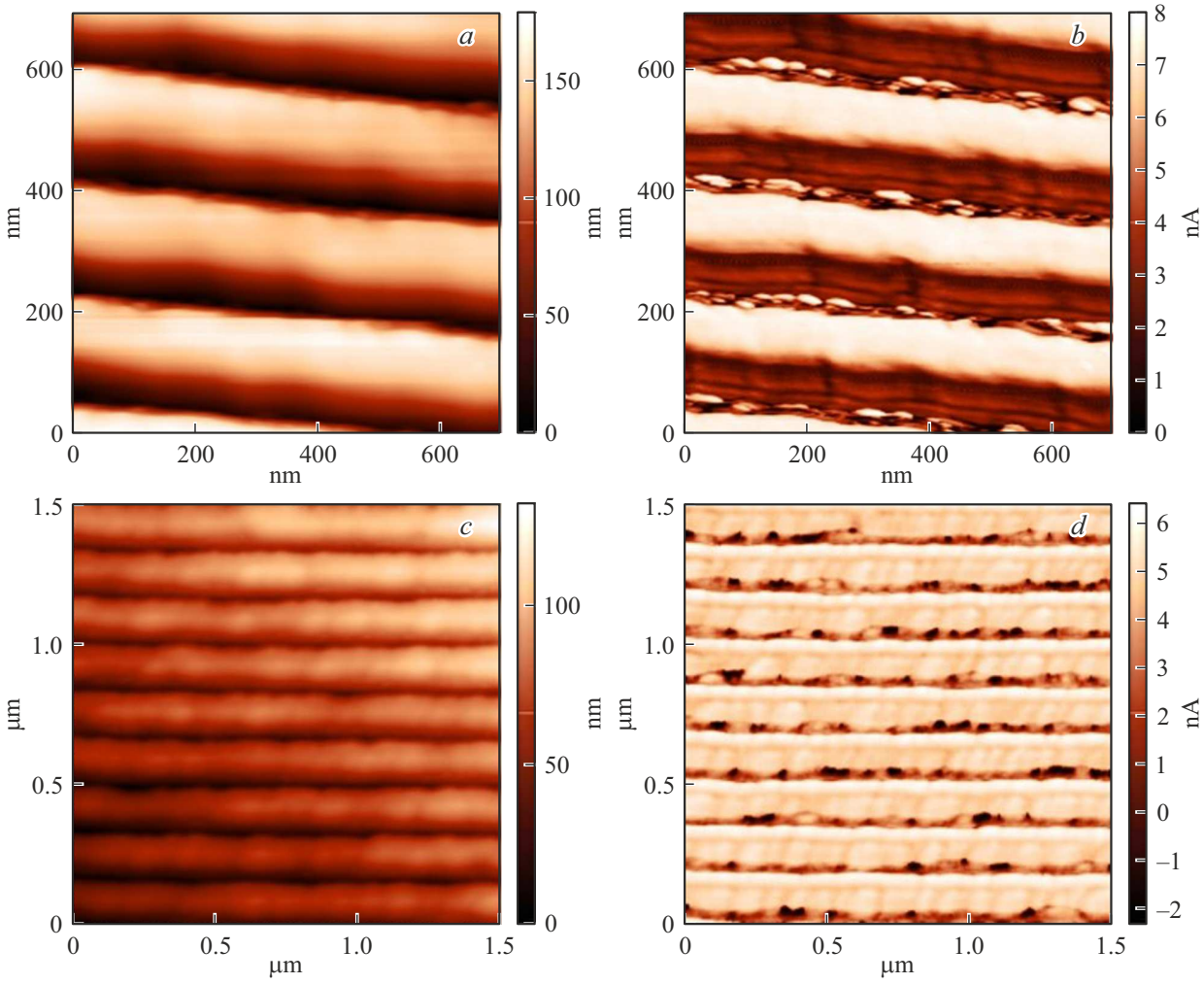

Figure 8. *a, c* — AFM and *b, d* — Mag*Sin images of the surface of gratings with G : h-BN nanoparticles deposited by 2D inkjet printing. *a, b* — Single printed layer, *c, d* — three printed layers.

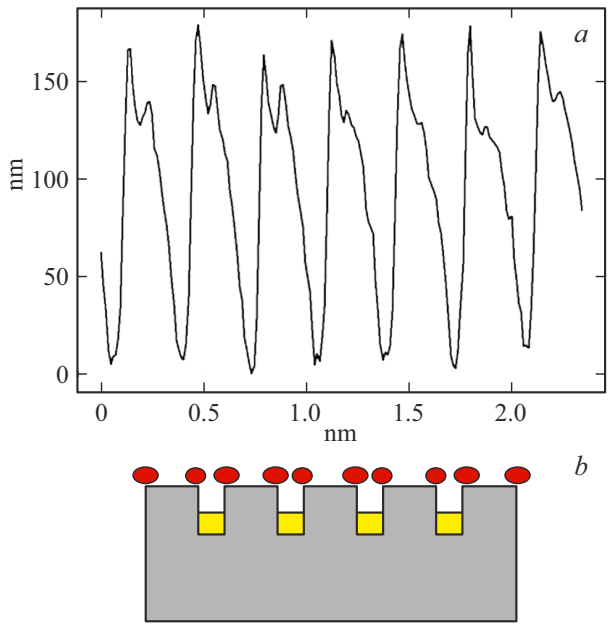

Figure 9. *a* — Transverse section profile of a nanostructured substrate with a layer of G:h-BN nanoparticles corresponding to triple-pass printing. *b* — corresponding schematic diagram of the distribution of G:h-BN nanoparticles over the activated grating surface.

The surface relief measured across the grating reveals that particles decorate the edges of arched polymer strips, forming 1D chains of composite particles. This was expected, since the barrier for physical adsorption of nanoparticles is lowered at the edges of steps due to local strain [19].

Sheet resistance $R = 50-70$ kOhm/sq was determined in conductivity measurements performed with a four-point probe head precisely along these chains; even a slight rotation of the sample resulted in a complete loss of conductivity. Figure 10 presents the current–voltage curves measured between silver contacts on the grating surface (several grating strips contributed to conduction) at various intercontact distances. The resistance of contacts was $R_c = 2-4$ Ohm/□.

The conductivity of G:h-BN particles on a structured and activated substrate is significantly higher (10–20 mA at a voltage of 1–2 V) than the one of FG:V_2O_5 nanoparticles. This is attributable to the fact that $3 \cdot 10^3$ nanoparticle chains were involved in measurements with Ag contacts ~ 300 mm in diameter; therefore, the current flowing along an individual chain may be estimated at $\sim 1\,\mu$A.

4. Discussion

Activation of polymer substrates is a well-known method of surface preparation for nanoparticle or film deposition. Specifically, plasma processing is a standard surface activation technique with its effect retained approximately over 30 min. This is not particularly convenient if different methods for structure fabrication are used. As was demonstrated above, activation in oxygen plasma resulted in grating distortion and filling of grooves. Long-term activation via gold sputtering and removal is of interest in terms of application of nanostructured substrates. It is likely that, from the physical standpoint, the surface is activated due to the presence of residual gold on the polymer surface after mechanical removal of a gold layer from the top of the grating. The activated polymer surface state, which enabled nanoparticle deposition with the formation of chains in the middle and at the edges of strips, persisted for at least several months of storage of these substrates.

Different types of positioning of nanoparticles (Figure 11) correspond to different regimes of nanoparticle interaction

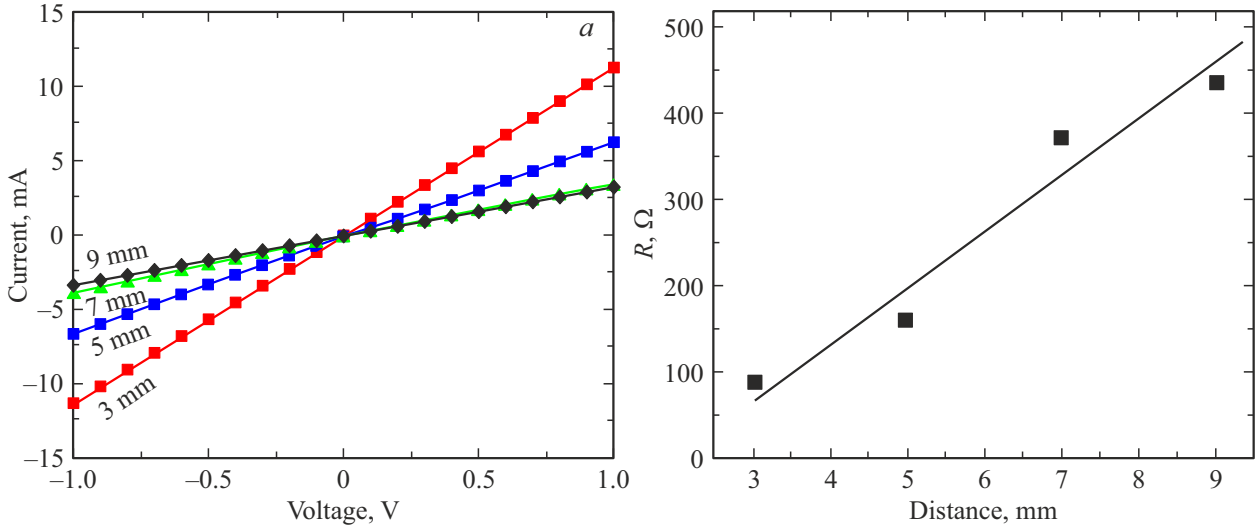

Figure 10. *a* — Current–voltage curves measured between silver contacts on the grating surface with deposited G:h-BN nanoparticles (three printed layers) at various intercontact distances (3–9 mm). The area of contacts was 0.09 mm^2. *b* — Dependence of resistance *R* on the distance between contacts.

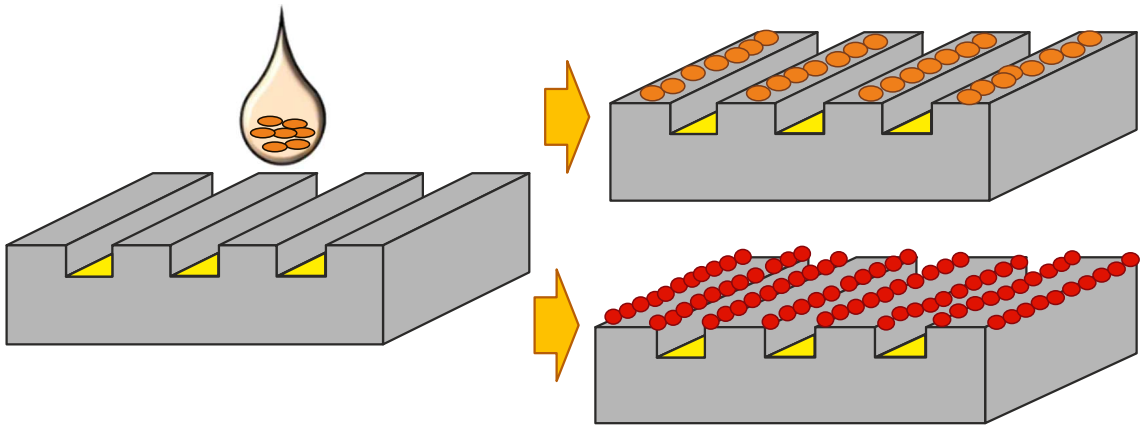

Figure 11. Schematic diagram of the FG : V_2O_5 (upper image) and G : h-BN (lower image) nanoparticle distributions over the activated grating surface.

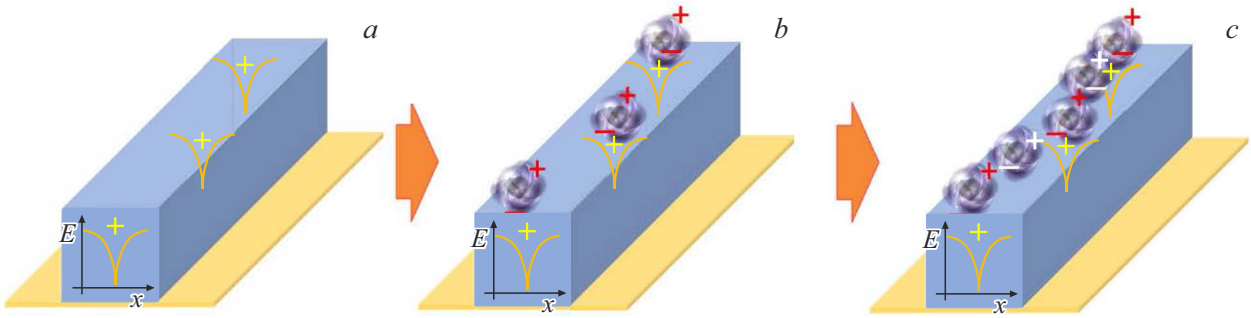

Figure 12. *a* — Schematic diagram of the activated polymer surface with electrically active centers; *b, c* — stages of formation of FG : V_2O_5 nanoparticle chains.

with the substrate. Characterizing the properties of FG : V_2O_5 nanoparticles, one should note that they have a hydrophilic surface (attributable to fluorinated graphene) and that FG films are characterized by a very low density of electrically active centers N_e ($N_e < 10^{10}\,\mathrm{cm}^{-2}$) and polarizability of V_2O_5 particles, which are crystalline hydrates and contain 2–3 water molecules [17]. Residual gold probably produces electrically active centers on the substrate surface, and a polarized FG : V_2O_5 particle may interact with such centers. Figure 12 presents the schematic diagram of an activated polymer surface and stages of formation of nanoparticle chains. It follows from Figure 5, where the positioning of FG : V_2O_5 nanoparticles (at their low concentration) reveals the positioning of electrically active centers, that these centers are distributed chaotically over the surface. it is worth noting individually that the thickness of FG particles (and, consequently, the potential barrier thickness) is ~ 2 nm. Attached particles are polarized and likely act as centers of chain formation by coupling with other nanoparticles.

As for particles of the second type (G : h-BN), we also have a multibarrier system, where potential barriers are associated with h-BN and have approximately the same width of ~ 2 nm [16]. Charge is not accumulated in this system: although barriers are present, graphene enables discharging. Under these conditions, the reduction in adsorption energy of particles at grating edges due to local strain takes center stage in interactions with the substrate [18]. In other words, the reactivity of polymer atoms is higher at deformed sites. Such changes may also be related to local strain in a nanoparticle driven by its specific morphology [19–21]. Composite G : h-BN particles form in a suspension and have a specific structure [16]. Atomic-level strain is a versatile tool for control and adjustment of structural and functional properties of nanomaterials in general and the adsorption energy of nanoparticles and their interaction with a surface in particular. This is the mechanism of formation of two chains of nanoparticles (see Figures 8 and 9) at the locally deformed edges of strips.

5. Conclusion

Structures formed by depositing two types of functional composite nanoparticles onto an intermediate polymer stamp grating, which was fabricated by imprint lithography, were studied. Composite G : h-BN nanoparticles and V_2O_5 particles coated with fluorinated graphene were deposited onto these substrates by 2D printing. If the polymer grating

surface is not activated, nanoparticles either rolled down into grooves or simply formed clusters and did no interact with the polymer surface. When the grating surface was activated with oxygen plasma, a solid nanoparticle coating was formed with filling of grating grooves and pointwise coalescence of grating strips. The process of sputtering of gold with its subsequent mechanical removal with an imprint lithography stamp was used for long-term activation of the polycarbonate-based grating surface. In the case of long-term surface activation, nanoparticles were positioned exclusively at the top of polymer strips (nanoridges) and did not reduce the grating relief depth. FG : V_2O_5 particles were arranged in the middle of polymer strips, while G : h-BN particles formed two chains along the edges of nanoridges. This is attributable to differences in the characteristics of nanoparticles and, consequently, in the nature of their interaction with the polymer substrate.

Acknowledgments

The authors would like to thank Dr. Sc. M.B. Shavelkina from the Joint Institute for High Temperatures of the Russian Academy of Sciences (Moscow) for providing them with graphene and boron nitride particles for fabrication of one type of nanoparticles.

Funding

This study was supported by grant 22-19-00191 from the Russian Science Foundation.

Conflict of interest

The author declares that he has no conflict of interest.

References

[1] D. Wang, Y. Mei, G. Huang. J Semicond. **39**, 011002 (2018).
[2] P. Cai, B. Hu, W.R. Leow, X. Wang, X.J. Loh, Y.-L. Wu, X. Chen. Adv. Mater. **30**, 1800572 (2018).
[3] H. Heidari, N. Wacker, R. Dahiya. Appl. Phys. Rev. **4**, 031101 (2017).
[4] T. Carey, S. Cacovich, G. Divitini, J. Ren, A. Mansouri, J.M. Kim, C. Wang, C. Ducati, R. Sordan, F. Torrisi. Nature Commun. **8**, 1202 (2017).
[5] A.A. Buchraiev, A.K. Zvezdin, A.P. Pyatakov, Yu.K. Fetisov. UFN **188**, 1288 (2018). (in Russian).
[6] I.V. Antonova. UFN **192**, 609 (2022). (in Russian).
[7] S. Zhou, J. Li, J. Lu, H. Liu, J.-Y. Kim, A. Kim, L. Yao, C. Liu, C. Qian, Z.D. Hood, X. Lin, W. Chen, T.E. Gage, I. Arslan, A. Travesset, K. Sun, N.A. Kotov, Q. Chen. Nature C **612**, 259 (2022).
[8] O.F. Silvestre, A. Rao, L.M. Liz-Marzán. Eur. J. Mater. **3**, 2202676 (2023).
[9] J. Dong, J.-F. Chen, M. Smalley, M. Zhao, Z. Ke, Y. Zhu, H.R. Tseng. Adv. Mater. **32**, 1903663 (2020).
[10] M. Hildebrand, F. Abualnaja, Z. Makwana, N. M. Harrison. J. Phys. Chem. C **123**, 4475 (2019).
[11] F. Yang, J. Feng, J. Chen, Z. Ye, J. Chen, D. K. Hensley, Y. Yin. Nano Research **16**, 5873 (2023).
[12] S. Jambhulkar, W. Xu, D. Ravichandran, J. Prakash, A.N.M. Kannan, K. Song. Nano Lett. **20**, 3199 (2020).
[13] V.A. Seleznev, V.S. Tumashev, H. Yamaguchi, V.Ya. Prinz. Prec. Eng. **82**, 316 (2023).
[14] O. Berezina, D. Kirienko, A. Pergament, G. Stefanovich, A. Velichko, V. Zlomanov. Thin Solid Films **574**, 15 (2015).
[15] N.A. Nebogatikova, I.V. Antonova, V.A. Volodin, V.Ya. Prinz. Physica E **52**, 106 (2013).
[16] I.V. Antonova, M.B. Shavelkina, D.A. Poteryaev, N.A. Nebogatikova, A.I. Ivanov, R.A. Soots, A.K. Gutakovskii, I.I. Kurkina, V.A. Volodin, V.A. Katarzhis, P.P. Ivanov, A.N. Bocharov. Adv. Eng. Mater. **24**, 2100917 (2022).
[17] A.I. Ivanov, V.Ya. Prinz, I.V. Antonova, A.K. Gutakovskii. Phys. Chem. Chem. Phys. **23**, 20434 (2021).
[18] Z. Wang, Y. Zhang, F. Liu. Phys. Rev. B **83**, 041403 (2011).
[19] D. Nelli, C. Roncaglia, C. Minnai. Adv. Phys. X, **8**, 2127330 (2023).
[20] M. Jørgensen, H. Grönbeck. Top. Catal. **62**, 660 (2019).
[21] M. Dupraz, N. Li, J. Carnis, L. Wu, S. Labat, C. Chatelier, Rim van de Poll, Jan P. Hofmann, Ehud Almog6, Steven J. Leake, Yves Watier, Sergey Lazarev, Fabian Westermeier, Michael Sprung, Emiel J.M. Hensen, Olivier Thomas, Eugen Rabkin, Marie-Ingrid Richard. Nature Commun. **13**, 3003 (2022)

Translated by D.Safin